

Physics

Electricity & Magnetism fields

Okayama University

Year 1999

Analysis of magnetic characteristics of
three-phase reactor made of
grain-oriented silicon steel

Takashi Kohsaka*

Norio Takahashi†

Shuichi Nogawa‡

Minoru Kuwata**

*Okayama University

†Okayama University

‡Nissin Electric Corporation, Limited

**Nissin Electric Corporation, Limited

This paper is posted at eScholarship@OUDIR : Okayama University Digital Information Repository.

http://escholarship.lib.okayama-u.ac.jp/electricity_and_magnetism/165

Analysis of Magnetic Characteristics of Three-Phase Reactor Made of Grain-Oriented Silicon Steel

Takashi Kohsaka, Norio Takahashi, *Fellow, IEEE*, Shuichi Nogawa, and Minoru Kuwata

Abstract—Flux and iron loss distributions of three-phase reactor are analyzed using the finite element method considering 2-D B - H curves and iron losses in arbitrary directions which are measured up to high flux density. It is shown that the total iron loss of reactor yoke does not change so much by the yoke dimension, although the local iron loss is increased when the width of yoke is decreased. The experimental verification of flux and iron loss distributions are also carried out.

Index Terms—Finite element method, grain-oriented silicon steel, reactor.

I. INTRODUCTION

IN THE ordinary reactor, the leg is made of grain-oriented silicon steel and yoke is made of nonoriented silicon-steel. To examine the possibility of using the grain-oriented silicon steel sheet in the yoke of three-phase reactor for improving the efficiency etc., it is necessary to analyze the flux and iron loss distributions in the reactor. By using the grain-oriented silicon steel, the size and weight may be reduced and but the estimation of iron losses of yokes is difficult because of butt joints between yokes and legs where the direction of flux is deviated from the rolling direction.

In this paper, the flux and iron loss distributions are analyzed using the finite element method which can take into account anisotropy [1]. 2-D B - H curves and iron losses in arbitrary directions which are measured up to 2 T are used in the analysis. The effect of yoke dimension on iron loss is examined, and the calculated flux waveforms and iron losses are compared with measured values.

II. MEASUREMENT OF 2-D MAGNETIC CHARACTERISTICS

The core of reactor which is examined in this paper is made of grain-oriented silicon steel (JIS:35G165). In order to measure the 2-D B - H curves and iron losses in arbitrary directions of grain-oriented silicon steel up to 2 T as shown in Figs. 1 and 2, an improved single-sheet tester, having H -coils in the x - and y -directions, is used [2]. The components of flux density (B_x , B_y) and magnetic field strength (H_x , H_y) in the rolling

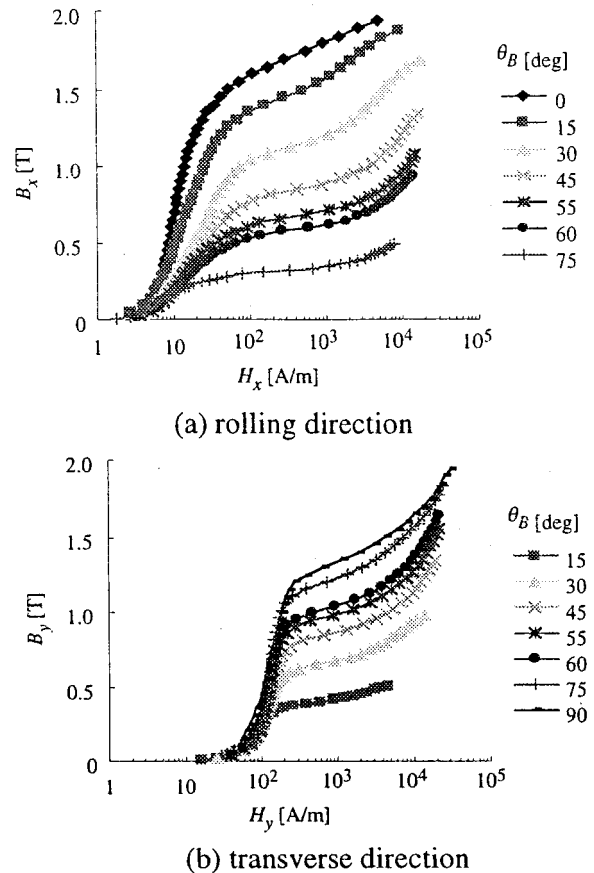


Fig. 1. 2-D B - H curves (35G165).

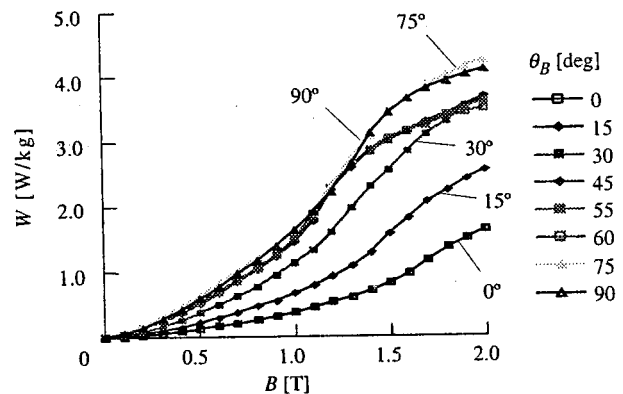


Fig. 2. 2-D iron loss curves (35G165).

and transverse directions are measured using various rectangular specimens which are cut in the θ_B directions. θ_B is the

Manuscript received October 25, 1999.

T. Kohsaka was with Department of Electrical and Electronic Engineering, Okayama University, 3-1-1 Tsushima, Okayama 700-8530, Japan. He is now with The Chugoku Electric Power Co., Inc, Japan.

N. Takahashi is with Department of Electrical and Electronic Engineering, Okayama University, 3-1-1 Tsushima, Okayama 700-8530, Japan (e-mail: norio@eplab.elec.okayama-u.ac.jp).

S. Nogawa and M. Kuwata are with Nissin Electric Co., Ltd., Kyoto 615-0906, Japan (e-mail: {nogawa; kuwata}@neonet.nissin.co.jp).

Publisher Item Identifier S 0018-9464(00)07183-1.

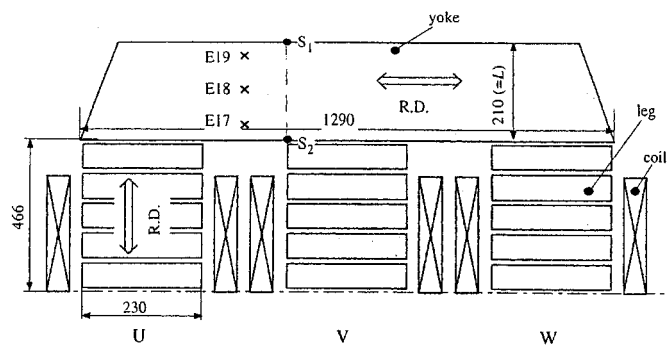


Fig. 3. Model of three-phase reactor.

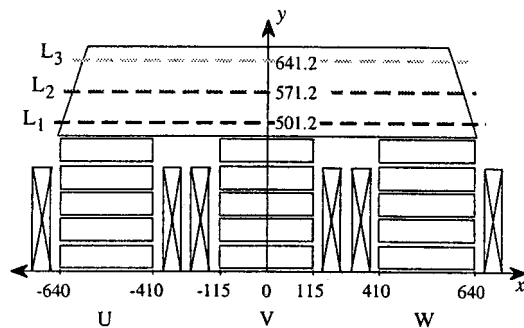


Fig. 4. Examined point.

direction of flux density vector from the rolling direction. A heatproof winding is used to excite until high flux density.

There are several ways to represent 2-D B - H curves, such as total B and H using θ_B and θ_{HB} (the angle between \mathbf{B} and \mathbf{H} vectors) [2]. For the convenience of the calculation method described in Chapter IV, B_x - H_x and B_y - H_y curves having parameter θ_B shown in Fig. 1 are used.

III. MODEL

Fig. 3 shows the analyzed model of three-phase reactor. The number of turns of winding is 333 and the frequency of power source is 50 Hz. The terminal voltage of the winding is 6072 V(rpm). The current in the winding is assumed as sinusoidal and the amplitude is determined so that the average flux density along S_1 - S_2 in Fig. 3 becomes nearly 1.4 T. The yoke width L is 210 mm.

If the edge of the yoke has a cut and the yoke width L is decreased, the reactor may become small and the weight can be reduced. Then, the effect of yoke width L on the flux and iron loss distributions is examined. In order to measure the flux density waveform in the yoke, search coils are set along the lines L_1 , L_2 and L_3 in Fig. 4 by making holes of 1 mm diameter in 17 sheets of silicon steel. Iron losses along the lines L_1 , L_2 and L_3 are measured by the initial temperature rise method using thermocouples.

IV. METHOD OF ANALYSIS

The flux distribution is analyzed using the 2-D B - H curves shown in Fig. 1. The coefficient, $\partial G_i^{(k)} / \partial A_j^{(k)}$, at the k th

 TABLE I
DISCRETIZATION DATA AND CPU TIME

yoke width L [mm]	190	200	210	220
number of nodes	2114			
number of elements	4140			
number of time steps	24			
number of nonlinear iterations per step (average)	1719	1714	1718	1709
CPU time [h]	44.7	44.1	45.1	48.7

computer used : VT-alpha (SPECfp 95 : 22.5)

convergence criterion of NR method : $\Delta A = 5.0 \times 10^{-3}$

nonlinear iteration in Newton-Raphson method can be represented by the following function:

$$\frac{\partial G_i^{(k)}}{\partial A_j^{(k)}} = g \left(\frac{\partial H_x^{(k)}}{\partial B_x^{(k)}}, \frac{\partial H_x^{(k)}}{\partial B_y^{(k)}}, \frac{\partial H_y^{(k)}}{\partial B_x^{(k)}}, \frac{\partial H_y^{(k)}}{\partial B_y^{(k)}} \right) \quad (1)$$

where g denotes a function. G_i and A_j are the residual compared with the analysis of isotropic material at a node i and the magnetic vector potential at a node j respectively. The coefficient matrix is unsymmetric due to $\partial H_x / \partial B_y$ and $\partial H_y / \partial B_x$. $\partial H_x / \partial B_y$ and $\partial H_y / \partial B_x$ in (1) are assumed to be zero. Only one B - H curve is used in an element during the Newton-Raphson iteration. Then, the new B - H curve is chosen corresponding the newly calculated θ_B . This process is iterated until the convergent results can be obtained. [1]. The B - H curve is calculated by interpolating the measured B - H curves stored in a computer.

As the convergence of the nonlinear analysis of magnetic field in such anisotropic material is not easy or, in the worst case, the solution does not converge, the modified Newton-Raphson (N.R.) method which introduces a relaxation factor [3] is used. Table I shows the discretization data, number of N.R. iterations, CPU time etc. Many N.R. iterations are necessary in the analysis of such anisotropic material compared with the analysis of isotropic material.

V. RESULTS AND DISCUSSION

A. Flux Density

Fig. 5 shows the flux distribution at the instant when the flux Φ_u in the U-leg is maximum. The flux flows along the yoke edge. This is the feature of anisotropic material [1].

Fig. 6 shows the comparison between the calculated and measured waveforms of the x -component of flux density at the points E17x and E18x in Fig. 3. Fig. 7 shows the distribution of maximum value of flux density along the lines L_1 , L_2 and L_3 shown in Fig. 4.

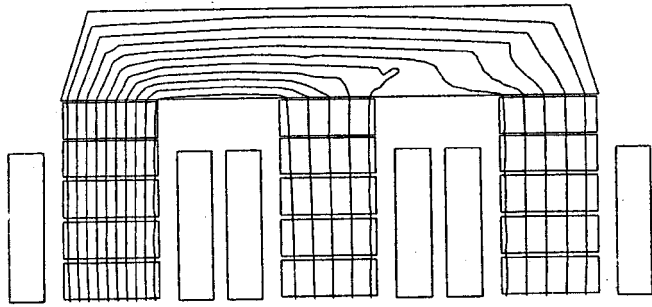
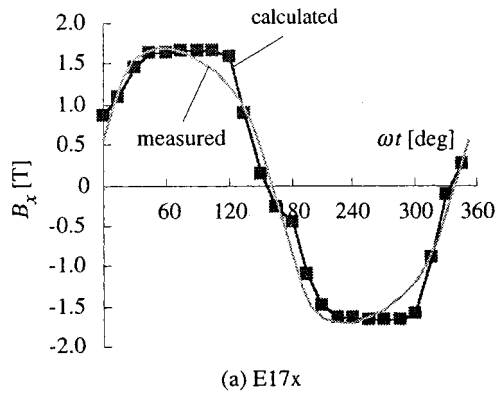
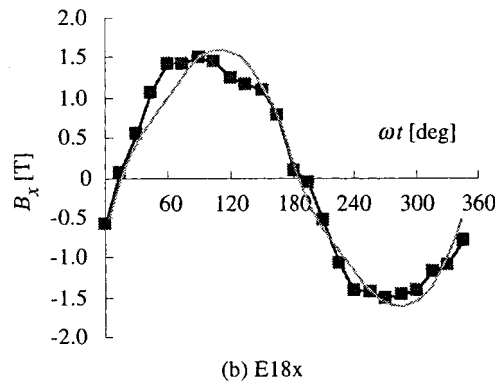


Fig. 5. Flux distribution (ϕu is maximum).



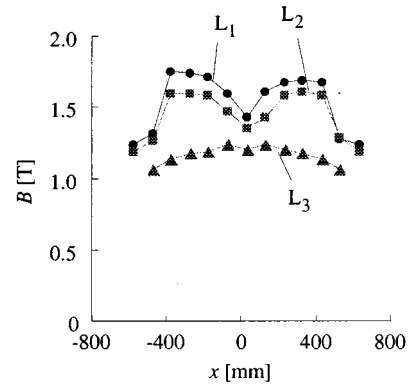
(a) E17x



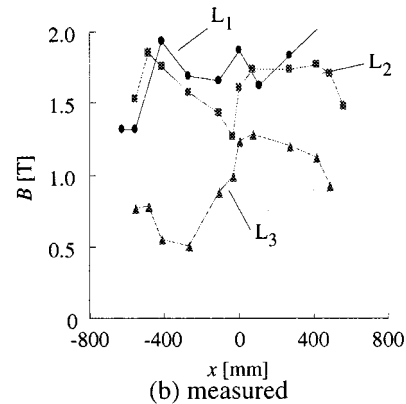
(b) E18x

Fig. 6. Flux waveforms ($L = 210$ mm).

The flux density in the middle part of yoke between legs is larger than that in the other part. The distribution of the measured maximum flux densities is not symmetrical with respect to y -axis due to the nonuniformity of material, difference of gap length in each leg, etc., and also due to measurement error. The discrepancy between the calculation and measurement may be due to the above-mentioned measurement error including the manufacturing uniformity, and also the insufficient number of measured B - H curves ($\theta_B = 0, 15, 30, 45, 55, 60$ and 75) shown in Fig. 1. This can be discussed as follows: The direction θ_B of flux density vector along the side of yoke is about 75 deg. B_x - H_x curve at $\theta_B = 75$ deg. is different from other B_x - H_x curve, such as $\theta_B = 60$ deg., very much. Therefore, B_x - H_x curve near $\theta_B = 75$ deg. which is interpolated using two nearest B_x - H_x curves may be different from the true B_x - H_x curve.



(a) calculated



(b) measured

Fig. 7. Distribution of flux density ($L = 210$ mm).

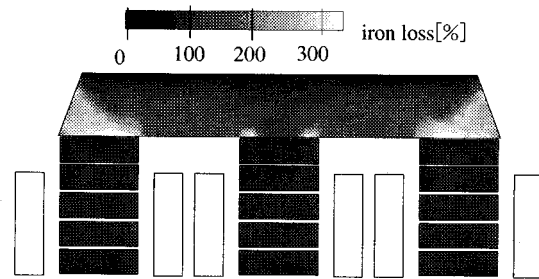


Fig. 8. Iron loss distribution ($L = 210$ mm, calculated).

B. Iron Loss

Fig. 8 shows the iron loss distribution calculated using the 2-D iron loss curves shown in Fig. 2. The average iron loss of the core $L = 210$ mm is normalized to 100%. The iron loss is calculated by assuming that the iron loss is the function of the absolute value B of the maximum ac flux density and the direction θ_B of flux density. The fact that the flux is nearly alternating is confirmed by plotting the locus of the calculated flux density vectors. Fig. 8 denotes that the iron loss is increased near both sides of yoke. This is because the direction of flux density vector is considerably deviated from the rolling direction near the side of yoke.

Fig. 9 shows the comparison of calculated and measured iron losses along the lines L_1, L_2 and L_3 . The sensors

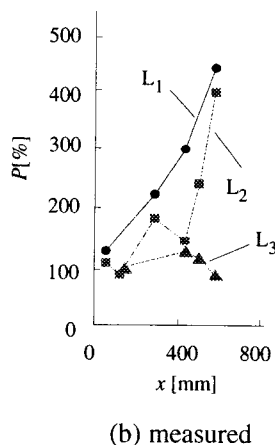
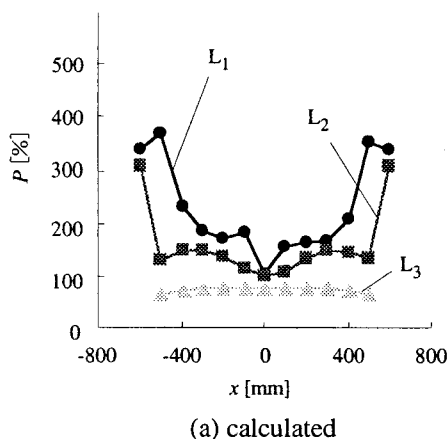


Fig. 9. Distributions of iron loss ($L = 210$ mm).

(thermocouple) for measuring iron losses are set only in the right hand side. The amplitude is different, but the tendency is similar.

Fig. 10 shows the total iron loss P , the average value $P^{(a)}$ and total weight of core W . The iron losses P and $P^{(a)}$ and the weight W at $L = 190$ mm are normalized to 100%. The total iron loss P is almost constant, because $P^{(a)}$ is decreased and W is increased with the width L of yoke.

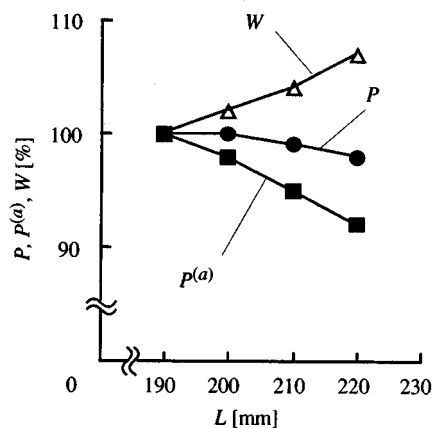


Fig. 10. Effect of yoke width L on iron loss (calculated).

VI. CONCLUSIONS

The obtained results can be summarized as follows:

- 1) 2-D $B-H$ curves and iron losses in arbitrary directions of grain-oriented silicon steel up to 2 T can be measured using the improved single-sheet tester. By using the above-mentioned data, acceptable calculated results which are near to measurement are obtained.
- 2) The effect of the yoke width on the flux and iron loss distribution is examined. As the total iron loss is scarcely affected by the yoke width, the yoke width can be reduced by taking account of the temperature rise.

The obtained results will give useful suggestions for the optimal design of reactor using the grain-oriented silicon steel.

ACKNOWLEDGMENT

The authors would like to thank Y. Sayama, director of Yasuda Industry Co., for preparing a part of measurement model.

REFERENCES

- [1] T. Nakata, K. Fujiwara, N. Takahashi, M. Nakano, and N. Okamoto, "An improved numerical analysis of flux distributions in anisotropic materials," *IEEE Trans. Magn.*, vol. 30, no. 5, pp. 3395-3398, 1994.
- [2] M. Nakano, H. Nishimoto, K. Fujiwara, and N. Takahashi, "Improvements of single sheet testers for measurement of 2-D magnetic properties up to high flux density," *IEEE Trans. Magn.*, vol. 35, no. 5, 1999.
- [3] K. Fujiwara, T. Nakata, N. Okamoto, and K. Muramatsu, "Method for determining relaxation factor for modified Newton-Raphson method," *IEEE Trans. Magn.*, vol. 29, no. 2, pp. 1962-1965, 1993.